Improving the Bioavailability and in Vitro Release of bovine liver Ferritin via Multi-Polymer microencapsulation system

Yaman S. Fadhil*[1], Sumyia K. Badawi[2], Taha M. T. Mohammed[2]

[1] Department of Veterinary public health, College of veterinary Medicine, University of Mosul, 41001, Mosul, Iraq

[2] Department of Food Science, College of Agriculture and Forestry, University of Mosul, 41001, Mosul, Iraq

Abstract

Although ferritin is considered biologically safe and a high iron source, its nature makes it vulnerable to degradation by stomach acid before its iron reaches the absorption sites in the intestine. This research aimed to examine the structural stability and functionality of a microencapsulation system composed of sodium alginate, whey protein isolate, and xanthan gum, to enhance the ferritin fortification of milk powder. Microcapsules were produced using extrusion and spray drying, and their morphology was investigated. The field emission scanning electron microscopy revealed a spherical shape with slight roughness on the nanoscale. The atomic force microscope show that the surface capsule has uniform distribution of peaks and valleys. In-vitro gastrointestinal digestion revealed that the microcapsules released 0.99 ppm of iron under the stomach condition, while most of the iron was released gradually under the intestine conditions (pH ≈ 7.5). Furthermore, the microencapsulation showed significant differences between the control sample and the high concentration of the ferritin-fortified sample in terms of the sensory evaluation. Therefore, the results indicate that the proposed microencapsulation multilayer is an effective system to produce iron fortified products with high bioavailability.

Keywords: Ferritin, Spray drying, Whey protein isolates, Xanthan gum, Sodium alginate.

Introduction

Iron is a trace element that has an important role in biological functions, and it is found in many cells like haemoglobin, cytochrome and etc. (Abbasi & Azari, 2011). Its deficiency can cause impaired cognitive functioning in children, reduced growth rate, adverse pregnancy outcomes, and diminished ability to work in adults (Derbyshire et al., 2010). Fortification of food is a successful approach for increasing iron intake (Tripathi & Platel, 2011). Conventional iron supplements can cause adverse reactions in the human body. Thus, it is important to explore and develop novel products with high iron bioavailability, better stability, and affordable cost.

Among several iron sources, ferritin a ubiquitous intracellular protein, stands out because of its ability to carry a high iron amount (up to 4500 iron atoms per molecule) and it has a good bioavailability in comparison to inorganic iron salts (Chiou & Connor, 2018). However, ferritin addition into milk products presents technical barriers. Ferritin is vulnerable to the low pH conditions of the gastric stage, where proteolytic enzymes and acidity can lead to its early degradation, resulting in reducing the amount of unaltered protein reaching the duodenal absorption loci (Perfecto et al., 2018). Moreover, iron fortification often initiates oxidative reactions, producing undesirable flavors and negative changes in the properties of the milk (Habeych et al., 2016). To overcome these barriers, micro-encapsulation is considered as a remarkable structure to shield the bioactive components from the processing conditions and the gastrointestinal conditions. Previous studies have emphasized the use of multilayer systems to improve the efficiency of encapsulation. Sodium alginate is used for its high ability to form gel via ionotropic gelation with Calcium chloride, but the nature porous of alginate beads causing a leakage of molecules (Ramos et al., 2018). Therefore, whey protein addition and xanthan gum create a more durable wall material, because whey protein offers film forming properties and xanthan gum provide a texture stabilizer and viscosity improving agent, enhancing the encapsulation efficiency (Khorshidi et al., 2021).

Since there is no information about microencapsulation of ferritin. Our study goal is to investigate the effect of ferritin microencapsulation using polymers like alginate, whey protein and xanthan gum on the iron bioavailability via in vitro gastrointestinal model.

Materials and Methods

2.1. Material:

Wall materials (Sodium alginate SA, xanthan gum XG and whey protein isolate WPI) were bought from the local market in Mosul city. Calcium chloride, potassium monophosphate, sodium chloride, pepsin, and bile salts were bought from the 1st lab company (Mosul, Iraq).

2.2 Microencapsulation and coating of Ferritin:

5 g of ferritin was added into 2% of sodium alginate solution and stirred gently for 30 min. Subsequently, the acquired suspension was introduced into a 1.5% calcium chloride solution by a sterile nozzle to form a ferritin-alginate beads. The collected beads isolated using centrifugation (3,700 g, 5 minutes) and afterwards washed with distilled water. Then, the beads were immersed in a second coating solution (4% whey protein isolate WPI, 0.4%

Xanthan gum XG) and mixed for 30 min, and moved into a container and was dried by spray drying method at 120°C. The coated microcapsule powder was collected, and its iron concentration was measured by Atomic Absorption spectrophotometer at lmax 248 nm (Khorshidi et al., 2021).

2.3 Morphology of the microcapsules:
The surface structure and the particle size of the capsule was assessed using scanning electron microscopy (MIRA III, Tehran, Iran) fitted with an energy dispersive X-ray analyzer. Atomic force microscope images were recorded using an ICON atomic force microscope (NaioAFM 2022, Nanosurf, Bagdad, Iraq) in tapping mode (Abdullah et al., 2023). X-ray diffraction patterns (PW1730, Tehran, Iran) were collected at room temperature using a powder diffractometer by scanning at a rate of 5°/min, in the range of 2Θ.

2.4 In-vitro digestion model:
The digestion simulation was followed as mentioned by (Fakri et al., 2026). Encapsulated ferritin was added at a ratio of 1:10 to the simulated gastric fluid, which was prepared by dissolving 1 g of NaCl solution in 100 mL of distilled water (w/v), adding 0.3 g/100 mL of pepsin, and adjusting the pH to 2.0 using HCl, and the solution was incubated for 2 h at 37 ºC. The remaining gastric fluid with the sample were transferred to the simulated intestinal fluid, which was prepared from 0.68 g of KH_2PO_4 in 19 mL of NaOH, followed by the addition of 100 mL of distilled water and then 2 g of bile salts. pH was adjusted to 7.5 and incubated for additional 2 hours at 37°C with light shaking. the Sample readings were taken at 0, 30, 60, 90, 120, 150, 180, 210, and 240 minutes and iron concentration in the sample was determined by AAS.

2.5 Fortification in milk
Capsulated ferritin was added to the skimmed milk powder (Regilait/France) at three different concentrations 190, 380 and 570 mg/25 g of powder milk, and mixed for 5 min for complete homogeneity of milk.

2.6 pH and Viscosity of Reconstituted Milk Powder:
The pH the reconstituted milk powder sample was tested using a pH meter by immersing the device's electrode into (Alani et al., 2026).
The viscosity was estimated using a viscometer following the method mentioned by (Alani et al., 2026), with some modifications. The R1 axial spindle was used with a 50 ml of the sample volume, and the spindle was left to rotate inside the sample at a speed of 150 for 60 seconds, then the apparent reading was taken on mPa.s.

2.7 Sensory evaluation:
Fifty trained faculty members, from the Department of Food Science, College of Agriculture and Forestry, University of Mosul, examined the sensory properties of the reconstituted milk powder, including taste, odor, taste, and overall acceptance, by a 9-point hedonic scale (Mousavi et al., 2019).

2.8 Statistical analysis:
Experiments were performed in triplicate. Data are presented as mean ± standard deviation. One-way ANOVA was used, and differences between means were tested using Duncan's multi-range test at a significance level of 0.05, using SPSS version 2022.

3 Results and Discussion

3.1 Iron concentration:
Iron content of the microencapsulated ferritin was determined using Atomic absorption spectrophotometry at 248 nm. The results of estimating the iron content in ferritin coated with sodium alginate, isolated whey protein, and xanthan gum, using atomic absorption spectrometry (AAS) at 248 nm, showed an iron concentration of 5.2 ppm based on the standard iron titration curve. After correction for a dilution factor of x10, this amounted to 52 ppm, equivalent to 52 mg/L in the 0.25 g coated ferritin sample used for analysis. Expressing the iron content per gram of coated ferritin, this equates to 26.32 mg/L.

3.2 Morphology of microcapsules:
Figure 1 reveals the results of scanning electron microscopy (SEM) analysis of the morphological characteristics of encapsulated ferritin. The micrographs reveal that the microcapsules are spherical to ovoid in shape with smooth surfaces at the microscale, indicating the formation of microcapsules free from fractures and cracks. Several grooves were observed, which is attributed to the use of spray drying encapsulation system and the biopolymers, which shrink when exposed to high temperatures due to moisture loss during the drying process. Furthermore, the micrographs did not reveal any visible cracks, gaps, or holes in the microcapsules, confirming their stability and the favorable molecular interactions between sodium alginate, isolated whey protein, and xanthan gum. This confirms that these factors contributed to the formation of a mechanically stable and flexible wall. Based on the 10 µm micrographs, the microcapsule sizes appear to be within the micrometer range. However, a variation in particle sizes is observed, and Figure 1 shows that the average particle diameter ranging from 2 to 30 µm. The distribution indicates that the majority of the capsules fall within the average size range of 10 to 25 µm, which suggests the most common capsule diameter in the ferritin-encapsulated sample. All these results confirm the success of the microcapsule manufacturing process.
Our results are consistent with the study by Montoya-Soto et al. (2025), where they conducted the encapsulation of two different antibiotics using WPI and Arabic gum (AG) via spray drying. They obtained spherical particles

with grooves on their surfaces, which they attributed to the spray drying conditions and the diffusion of water from inside the microcapsules due to heat, creating a pressure difference between the inside and outside of the microcapsule.

The finding by Rajam et al. (2012) also supports our results as they have found that the smooth surface of the capsules and the absence of any fractures indicate the behavior of the isolated whey protein WPI to reduce the roughness of the microcapsule surface, and the prevention of the degradation or loss of the base material.

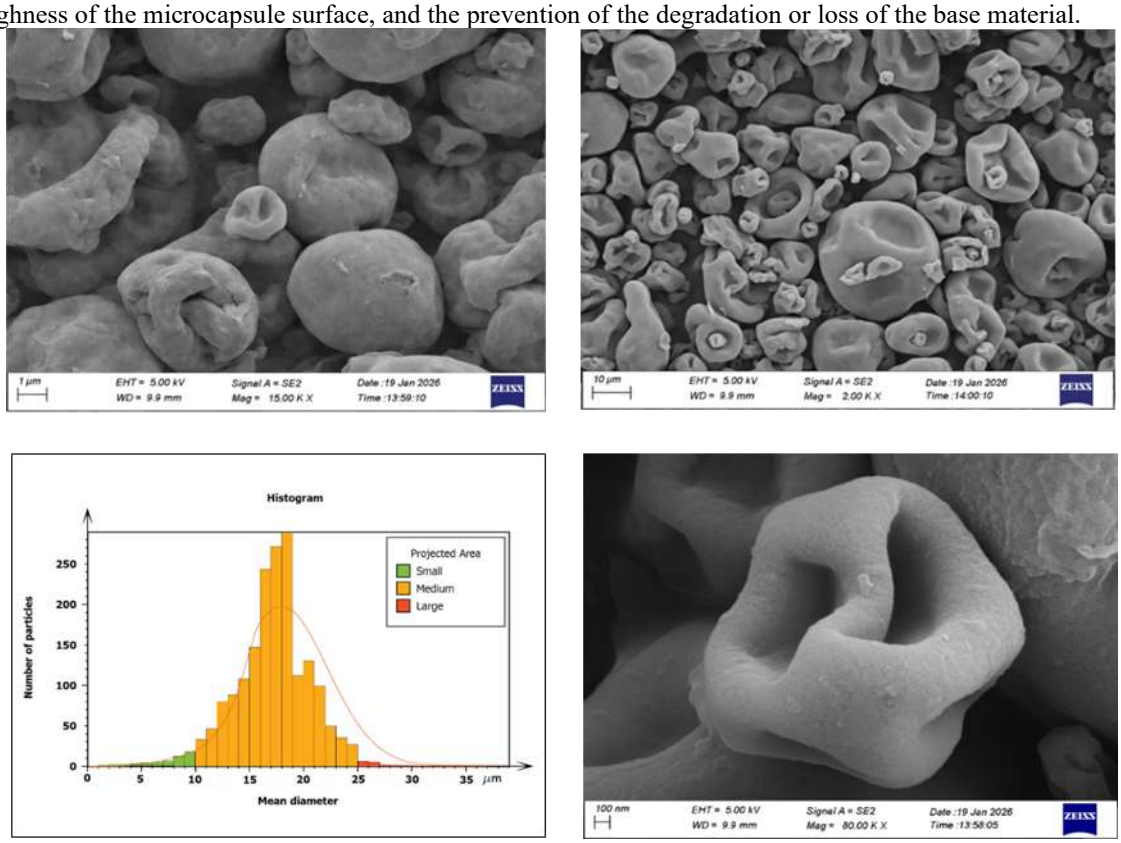

Figure (1) FESEM technique for studying the surface structure and general shape characteristics of the encapsulated microcapsules of ferritin protein.

Figure (2) shows the atomic force microscopy (AFM) results of three-dimensional topographic images scanned over a 4 x 4 µm area of microcapsules prepared from sodium alginate, isolated whey protein, and xanthan gum using extrusion and spray-drying techniques. Figure (2-A) shows the surface topography of the microcapsules, with values ranging from -4.1 to +16.9 nm, while the maximum height (Sz) reached approximately 21 nm. The average surface roughness (Sa) was approximately 9.35 nm. These values indicate the presence of nanoscale peaks and depressions, confirming that the microcapsule surface is rough at the nanoscale rather than perfectly smooth. Figure (2-B) shows the distribution of the surface topography. A uniform distribution of peaks is observed across the scanned area, with no heterogeneous distribution of the coating materials. The bright areas represent peaks, while the dark areas represent surface depressions. This corresponds to the autocorrelation length (Sal), which was approximately 494.3 nm, indicating a homogeneous distribution of nanostructures across the capsule surface, extending for a distance of approximately half a micrometer. Figure (2-C) provides a detailed visual representation of the capsule surface, showing a greater number of peaks (relatively similar in height) compared to fewer surface depressions. This suggests that the presence of these peaks corresponds to skewness (Ssk) deviation of approximately 0.46 nm, where the Ssk deviation is a determining factor for the surface content of the capsules.

Similar results are found by Zhang et al. (2022), who prepared microcapsules using sodium alginate and isolated whey protein and studied their surface structure. They found that these materials resulted in capsules with a uniform surface and improved capsule stability, which aligns with our findings of a relatively homogeneous surface. In addition, Vinceković et al. (2024) stated that the addition of milk proteins modifies roughness values surface patterns, as it can increase roughness according to the composition, which is consistent with slight differences in elevations while the surface remains homogeneous.

Figure 3 reveals the finding of the energy dispersive X-ray spectroscopy analysis of the encapsulated ferritin. The analysis reveals that carbon and oxygen are present as the dominant elements, comprising approximately 85% of the total content. The intensity of these elements indicates that the encapsulating material is an organic polymer, consistent with the structure of polysaccharide-protein biopolymers. This structure also suggests the presence of functional groups such as hydroxyl-OH and carboxyl-COOH, which contribute to the cohesion of the capsule structure and protect the ferritin protein. This aligns with the findings of Wang et al. (2022) regarding the encapsulation of L. plantarum bacteria with alginate and isolated whey protein. The figure also shows the presence of sodium, as sodium ions naturally bind to alginate molecules. Furthermore, the detection of calcium indicates successful ionic bonding between calcium ions and alginate chains. This reaction is responsible for the build-up of a stable gel network, which strengthens microcapsule structure. Other elements, such as chlorine (Cl) and sulfur

(S), were also present, likely originating from the preparation solutions or the coating materials used. The iron (Fe) peak was observed only in the high-energy region at 6.3 KeV. This strongly suggests that the ferritin protein was successfully encapsulated within the microcapsules, as X-ray spectroscopy is a near-surface analytical technique, typically used in regions up to 2 µm in diameter. These results indicate the successful formation of stable microcapsules capable of protecting the ferritin protein from gastric conditions.

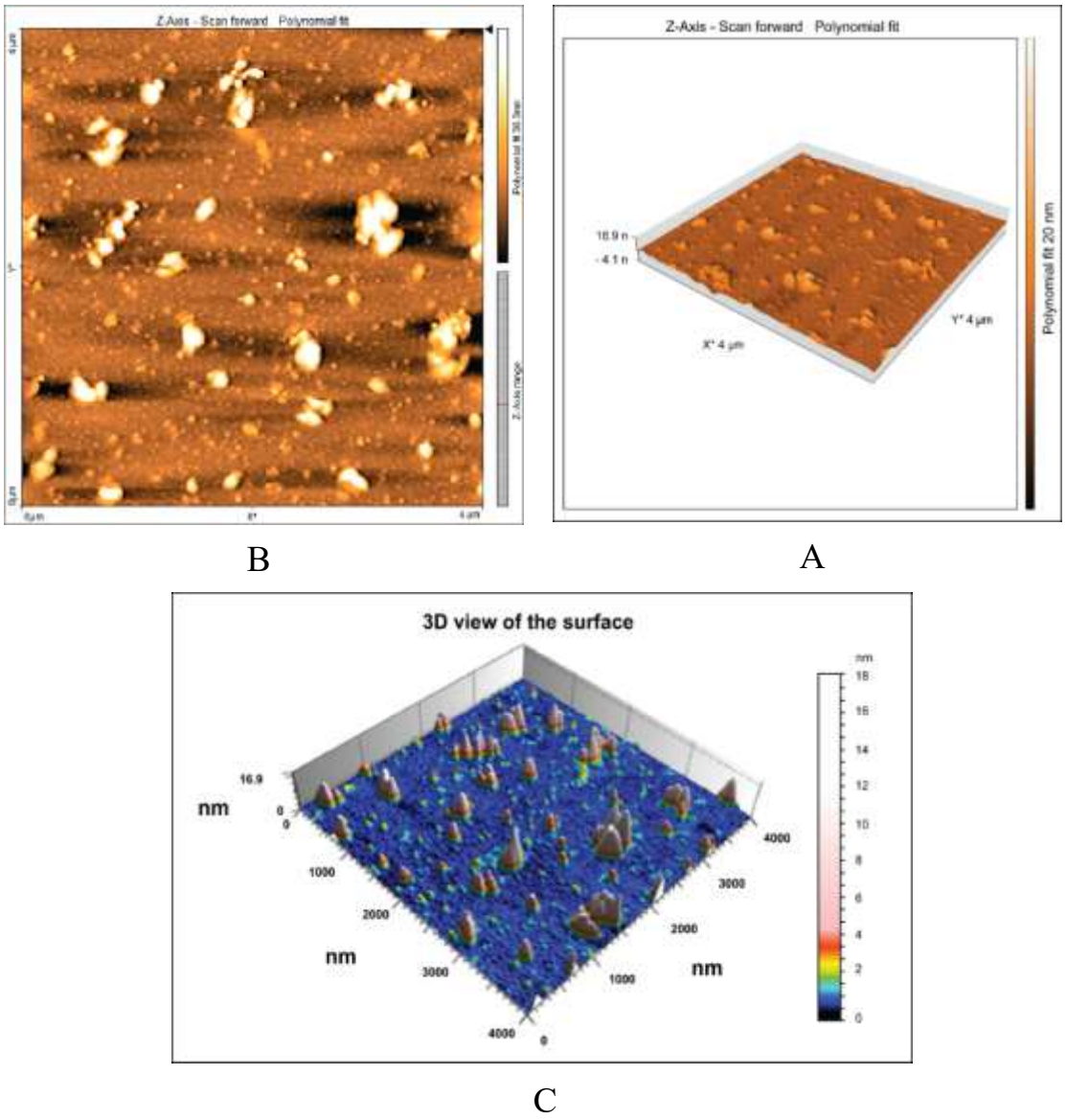

Figure (2) Atomic force microscope for evaluating the surface structure of microcapsules.

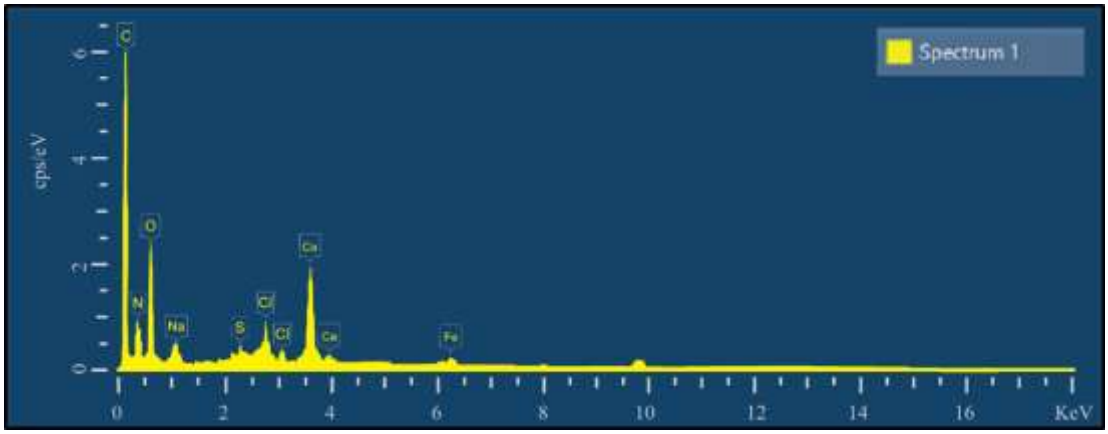

Figure (3) Energy-dispersive X-ray spectrum of encapsulated ferritin protein.

Figure 4 shows the results of X-ray diffraction analysis of the ferritin. The pattern shows a diffraction peak at 2θ angles centered at 20.6°, with an intensity ranging from 800 to 1200 count units. The appearance of this peak at 20° indicates the presence of ordered crystalline regions, a characteristic feature of polysaccharide and protein-

based coating polymers. The pattern also shows broadly extended peaks, which in turn indicates that the capsules have an amorphous structure. The semi-crystalline structure observed in the pattern is attributed to the interactions between the polymer's molecules like the hydrogen bonds, which form limited, ordered crystalline regions within the amorphous capsule structure. Similar results have found by of Sharifi et al. (2021), who found that polysaccharide-based coating polymers, such as gum arabic with whey proteins, exhibit a semi-crystalline arrangement indicating the bonding of wall materials within a two-phase structure. This structure enhances the protective and isolating properties of the encapsulated materials and increases the structural stability of the microcapsules. Luo et al. (2022) also noted that semi-crystalline coating systems enhance the protection of the active ingredient from thermal stress and gastrointestinal conditions, observations that support the findings of this study.

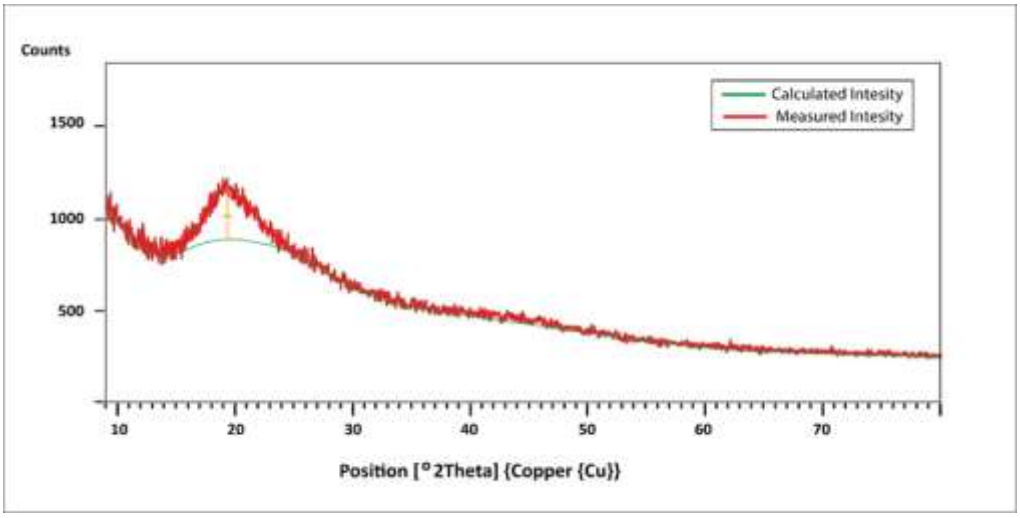

Figure (4) X-ray diffraction (XRD) analysis of ferritin microcapsules

Figure 5 shows the UV-Vis spectroscopic analysis results of the coated ferritin sample. The figure reveals distinct peaks in the UV-Vis region (200–400 nm), with the absorption peak appearing at 276 nm at a value of 1.109 AU. This absorption at 280 nm is reported to the presence of aromatic amino acids such as tryptophan, which are present in the protein structure. Since ferritin and the isolated whey protein WPI are protein compounds, this peak reflects electron transitions in the aromatic acids occurring in the 260–280 nm range. Our finding is in agreement with those reported by Meng et al. (2022), who observed major absorption peaks for the isolated whey protein WPI in the 220–280 nm range, a finding they linked to the presence of peptide bonds and aromatic amino acid.

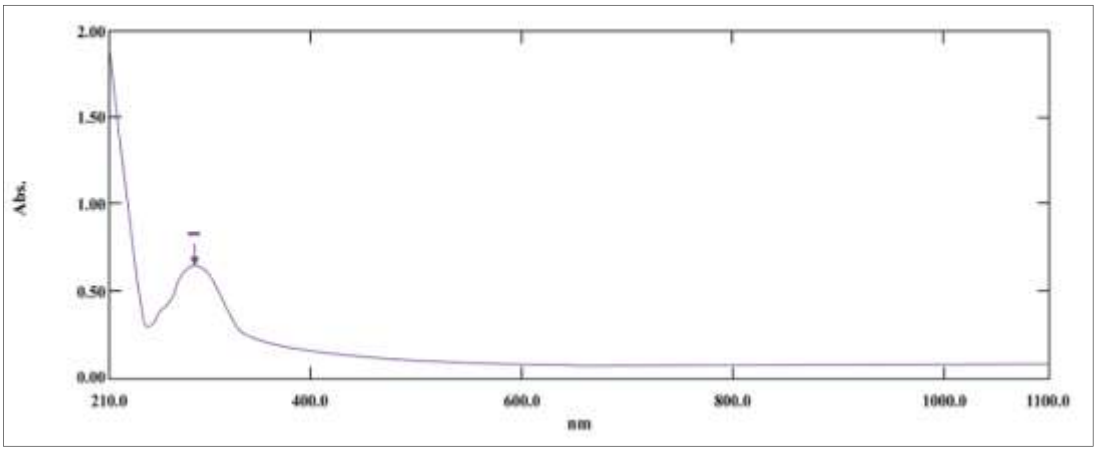

Figure (5) Ultraviolet-visible (UV-VIS) spectrum of the encapsulated ferritin.

Gastric and intestinal release:

Figure 6 show the iron release from the encapsulated ferritin. The microcapsules throughout the initial 2 hours in SGF exhibited high durability, which lead to an iron release reached 0.99 ppm at the 120 minutes. This confirms that the most of the ferritin remained inside the capsules. We attributed the minimal release in the gastric stage to the alginate's properties. At gastric pH, the alginate's carboxylate groups undergo gaining proton to form alginic acid, which form a tight, insoluble layer and shrinkage of the microcapsule matrix (Zhang et al., 2016). This shrinkage makes the porosity of the beads so tiny, effectively locking the ferritin inside and preventing it from hydrolysis by pepsin enzyme. Additionally, the coating materials of WPI and XG give excess protection to the porosity of the beads and prevent the iron release in the stomach. Therefore, reducing the risk for gastric irritation and nausea that associated with iron supplementation (Lin et al., 2021).

However, upon transferring the microcapsules to SIF, a rapid increase in release rate was observed. A burst release happened during the first half hour reaching 2.05 ppm in the intestinal stage, followed by a gradual release,

reaching a 6.92 ppm by the end of the digestion simulation. The high release during the intestinal stage is caused by the increase in pH 7.5 above the pKa of alginate, which caused the loss of a proton from the carboxyl groups, restoring the soluble alginate form. This leads to a strong electrostatic rejection between the polymer chains, leading to a significant swelling and breakdown of the polymer matrix (Malektaj et al., 2023).

Figure (6) In vitro release profile of iron under simulated gastrointestinal conditions.

3.4 Rheological properties of the reconstituted powders:

Table 1 shows the pH results for the fortified powder milk. No significant differences (P>0.05) in pH values found between the control and fortified samples. The stable pH values around 6.6 are a positive indicator of the efficiency of the encapsulation process in isolating iron from the milk medium, thus preventing oxidation or hydrolysis reactions that could lead to the release of hydrogen ions or a change in the product's acidity immediately after preparation. These finding support what Khorshidian et al. (2021) found in their study on fortifying yogurt with Lactobacillus acidophilus bacteria, encapsulated with sodium alginate and coated with isolated whey protein and xanthan gum. They observed no significant differences in the pH of yogurt containing encapsulated L. acidophilus compared to plain yogurt (without probiotics).

However, for the viscosity results showed a significant and progressive increase (P<0.05) in the viscosity values of the enriched samples, rising from 1.58 mPa.s in the control sample to 1.79 mPa.s at the highest concentration. This increase is directly associated with the rheological properties of the polymers used, specifically xanthan gum and alginate. Xanthan gum is known for its high water absorption capacity and ability to form a viscous network even at low concentrations, while alginate possesses thickening properties, leading to increased resistance to flow and a higher viscosity reading. Our results agree with that of Khorshidian et al. (2021), who reported that adding capsules coated with a combination of whey proteins and polysaccharides added to yogurt caused a significant increase in viscosity and consistency. Their study attributed this to xanthan gum's ability to modify rheological properties and bind water molecules, thus altering the consistency of the liquid or semi-liquid product towards increased viscosity.

Table 1: Effect of milk fortification with encapsulated ferritin on its physical properties.

Parameters	**Iron Concentration (mg/25 g fortified milk)**			
	0	**5**	**10**	**15**
pH	6.63 ± 0.023 a	6.62 ± 0.004 a	6.61 ± 0.012 a	6.61 ± 0.016 a
Viscosity (mPa.s)	1.58 ± 0.13 c	1.62 ± 0.09 bc	1.65 ± 0.11 b	1.79 ± 0.34 a

Values are expressed as mean ± standard deviation. Means within the same row followed by different letters (a, b) are significantly different ($p < 0.05$).

3.5 Sensory evaluation:

Table 2 shows the results of fortifying milk with encapsulated ferritin on its sensory properties. Although all parameters maintained a high acceptance range (≥8 on a 9-point scale), significant differences were observed in the color and overall acceptance parameters between the control sample and the fortified milk sample with 1.493g encapsulated ferritin. These differences are mainly linked to the increase in total solids components, also the scattering of light rays reflected from the surface of the milk, which eventually effect on the score of the overall acceptance. Other than this all parameters maintained a high acceptance range (≥8 on a 9-point scale) this indicate that the multilayer wall acted as a barrier that limited the interaction between the ferritin and the milk components, which resulted in reducing oxidative, volatile formation. Also, the metallic off-flavors related to iron fortification

were not identified, similar results in previous studies found that microencapsulation significantly improves palatability of iron-fortified foods (Gupta et al., 2015)

Table 2: Effect of milk fortification with encapsulated ferritin on its sensory properties.

Iron Concentration (mg/250 ml)	Parameters			
	Color	Odor	Taste	Overall acceptance
0	9.00 ± 0.000 a	9.00 ± 0.000 a	9.00 ± 0.000 a	9.00 ± 0.000 a
5	8.66 ± 0.033 ab	9.00 ± 0.000 a	9.00 ± 0.000 a	8.66 ± 0.033 ab
10	8.66 ± 0.033 ab	9.00 ± 0.000 a	9.00 ± 0.000 a	8.66 ± 0.033 ab
15	8.33 ± 0.066 b	8.66 ± 0.033 a	8.66 ± 0.033 ab	8.33 ± 0.066 b

Values are expressed as mean ± standard deviation. Means within the same column followed by different letters (a, b) are significantly different ($p < 0.05$).

Conclusion

Micro-capsulation is a promising technology for protect ferritin and allow for full control release of its iron. In our study, the results exhibited that the use of multilayer system of alginate/whey protein isolate and xanthan gum is an effective strategy to protect ferritin from breaking down under simulated gastric conditions and allow the majority of its iron to be released in the small intestine near its absorption sites. The microcapsules showed a controlled and gradual release of ferritin under the intestinal stage. Furthermore, the polymers helped in maintaining the pH and viscosity of the milk, also did not allow any negative effect on the sensory characteristic of the reconstituted milk powder even at a higher level, preserving quality while enabling nutritional enhancement.

Acknowledgment

The researchers express their gratitude to the University of Mosul, College of Agriculture and Forestry / Department of Food Sciences, for providing the necessary materials and allowing the use of its scientific laboratory facilities.

CONFLICT OF INTEREST: The authors report no conflicts of interest and responsible for the content and writing of the paper.

References

1. Abbasi, S., & Azari, S. (2011). Efficiency of novel iron microencapsulation techniques: fortification of milk. International Journal of Food Science and Technology, 46(9), 1927e1933. https://doi.org/10.1111/j.1365-2621.2011.02703.x.
2. Abdullah, E. A., Badawi, S. K., & Jafar, N. B. (2023, December). Evaluation of Antibacterial Activity of Selenium and Copper Oxide Nanoparticles Synthesized by Hibiscus sabdariffa L. Extract. In IOP Conference Series: Earth and Environmental Science (Vol. 1262, No. 6, p. 062043). IOP Publishing. https://doi.org/10.1088/1755-1315/1262/6/062043
3. Alani, A. A., Mohammed, T. M. T., & Badawi, S. K. (2026). SIMULATION OF THE SURVIVAL OF LACTOBACILLUS PLANTARUM IN THE GASTROINTESTINAL TRACT ENCAPSULATED WITH SODIUM ALGINATE USING THE EMULSIFICATION-SPRAY DRYING TECHNIQUE. Mesopotamia Journal of Agriculture, 54(1), 59. https://doi.org/10.33899/mja.2026.163080.1666
4. Chiou, B., & Connor, J. R. (2018). Emerging and dynamic biomedical uses of ferritin. Pharmaceuticals, 11(4), 124. https://doi.org/10.3390/ph11040124.
5. Derbyshire, E., Brennan, C. S., Li, W., & Bokhari, F. (2010). Iron deficiency e is there role for the food industry? International Journal of Food Science & Technology, 45(12), 2443e2448. https://doi.org/10.1111/j.1365-2621.2010.02431.x.
6. Fakri, T. Y., Badawi, S. K., & Mustafa, Y. F. (2026). Calcium and vitamin D3 fortification of almond milk: A chemical engineering approach to enhancing nutritional quality and mineral bioavailability. Applied Chemical Engineering, 9(2), 59. ACE-5989.
7. Gupta, C., Chawla, P., & Arora, S. (2015). Development and evaluation of iron microencapsules for milk fortification. CyTA-Journal of Food, 13(1), 116-123. https://doi.org/10.1080/19476337.2014.918179
8. Habeych, E., van Kogelenberg, V., Sagalowicz, L., Michel, M., & Galaffu, N. (2016). Strategies to limit colour changes when fortifying food products with iron. Food Research International, 88, 122-128. https://doi.org/10.1016/j.foodres.2016.05.017.
9. Khorshidi, M., Heshmati, A., Taheri, M., Karami, M., & Mahjub, R. (2021). Effect of whey protein-and xanthan-based coating on the viability of microencapsulated Lactobacillus acidophilus and physiochemical, textural, and sensorial properties of yogurt. Food Science & Nutrition, 9(7), 3942-3953. https://doi.org/10.1002/fsn3.2398.

10. Lin, D., Kelly, A. L., Maidannyk, V., & Miao, S. (2021). Effect of structuring emulsion gels by whey or soy protein isolate on the structure, mechanical properties, and in-vitro digestion of alginate-based emulsion gel beads. Food Hydrocolloids, 110, 106165. https://doi.org/10.1016/j.foodhyd.2020.106165.
11. Luo, X., Fan, S., He, Z., Ni, F., Liu, C., Huang, M., Cai, L., Ren, G., Zhu, X., Lei, Q., Fang, W., & Xie, H. (2022). Preparation of alginate-whey protein isolate and alginate-pectin-whey protein isolate composites for protection and delivery of Lactobacillus plantarum. Food Research International, 161, 111794. https://doi.org/10.1016/j.foodres.2022.111794
12. Malektaj, H., Drozdov, A. D., & deClaville Christiansen, J. (2023). Swelling of homogeneous alginate gels with multi-stimuli sensitivity. International Journal of Molecular Sciences, 24(6), 5064. https://doi.org/10.3390/ijms24065064.
13. Meng, Y., Xue, Q., Chen, J., Li, Y., & Shao, Z. (2022). Structure, stability, rheology, and texture properties of ε-polylysine-whey protein complexes. Journal of Dairy Science, 105(5), 3746–3757. https://doi.org/10.3168/jds.2021-21219
14. Montoya-Soto, J. G., González-Laredo, R. F., Medina-Torres, L., Gallegos-Infante, J. A., Ochoa-Martínez, L. A., & Manero, O. (2025). Probiotic microencapsulation by spray drying using Aloe vera (Aloe Barbadensis Miller) mucilage, whey protein isolates and gum arabic as encapsulation agents. CyTA-Journal of Food, 23(1), 2587498. https://doi.org/10.1080/19476337.2025.2587498
15. Perfecto, A., Rodriguez-Ramiro, I., Rodriguez-Celma, J., Sharp, P., Balk, J., & Fairweather-Tait, S. (2018). Pea ferritin stability under gastric pH conditions determines the mechanism of iron uptake in Caco-2 cells. The Journal of Nutrition, 148(8), 1229-1235. https://doi.org/10.1093/jn/nxy096.
16. Rajam, R., Karthik, P., Parthasarathi, S., Joseph, G. S., & Anandharamakrishnan, C. J. J. O. F. F. (2012). Effect of whey protein–alginate wall systems on survival of microencapsulated Lactobacillus plantarum in simulated gastrointestinal conditions. Journal of Functional Foods, 4(4), 891-898. https://doi.org/10.1016/j.jff.2012.06.006
17. Ramos, P. E., Cerqueira, M. A., Teixeira, J. A., & Vicente, A. A. (2018). Physiological protection of probiotic microcapsules by coatings. Critical Reviews in Food Science and Nutrition, 58, 1864–1877. https://doi.org/10.1080/10408 398.2017.1289148.
18. Sharifi, S., Rezazad-Bari, M., Alizadeh, M., Almasi, H., & Amiri, S. (2021). Use of whey protein isolate and gum Arabic for the co-encapsulation of probiotic Lactobacillus plantarum and phytosterols by complex coacervation: Enhanced viability of probiotic in Iranian white cheese. Food Hydrocolloids, 113, 106496. https://doi.org/10.1016/j.foodhyd.2020.106496
19. Tripathi, B., & Platel, K. (2011). Iron fortification of finger millet (Eleucine coracana) flour with EDTA and folic acid as co-fortificants. Food Chemistry, 126(2), 537e542. https://doi.org/10.1016/j.foodchem.2010.11.039
20. Vinceković, M., Živković, L., Turkeyeva, E., Mutaliyeva, B., Madybekova, G., Šegota, S., ... & Kajić, S. (2024). Development of Alginate Composite Microparticles for Encapsulation of Bifidobacterium animalis subsp. lactis. Gels, 10(11), 752. https://doi.org/10.3390/gels10110752
21. Wang, X., Gao, S., Yun, S., Zhang, M., Peng, L., Li, Y., & Zhou, Y. (2022). Microencapsulating alginate-based polymers for probiotics delivery systems and their application. Pharmaceutics, 15(5), 644. https://doi.org/10.3390/ph15050644
22. Xin, M., Zhao, M., Tian, J., & Li, B. (2023). Guidelines for in vitro simulated digestion and absorption of food. Food Frontiers, 4(1), 524-532. https://doi.org/10.1002/fft2.186
23. Zhang, Z., Zhang, R., Zou, L., & McClements, D. J. (2016). Protein encapsulation in alginate hydrogel beads: Effect of pH on microgel stability, protein retention and protein release. Food Hydrocolloids, 58, 308-315. https://doi.org/10.1016/j.foodhyd.2016.03.015.